Citation of the present book chapter

Cruzado, A., Bernardello, R., Ahumada-Sempoal, M.A., Bahamon, N. 2012. Modelling the Pelagic Ecosystem Dynamics: The NW Mediterranean. *In* Marine Ecosystems, 35-60 pp. Ed. by A. Cruzado. InTech Open Access Publisher. Rijeka, Croatia. 310 pp.

Marine Ecosystems
Edited by Antonio Cruzado

Published by InTech
Janeza Trdine 9, 51000 Rijeka, Croatia

Publishing Process Manager Daria Nahtigal
Technical Editor Teodora Smiljanic
Cover Designer InTech Design Team

First published February, 2012
Printed in Croatia

A free online edition of this book is available at www.intechopen.com
Additional hard copies can be obtained from orders@intechweb.org

Marine Ecosystems, Edited by Antonio Cruzado
p. cm.
ISBN 978-953-51-0176-5

2

Modelling the Pelagic Ecosystem Dynamics: The NW Mediterranean

Antonio Cruzado[1,*], Raffaele Bernardello[2],
Miguel Ángel Ahumada-Sempoal[3] and Nixon Bahamon[4]
[1]*Oceans Catalonia International SL,*
[2]*Earth and Environmental Science, University of Pennsylvania,*
[3]*Resources Institute, University del Mar,*
[4]*Center for Advanced Studies of Blanes (CEAB-CSIC),*
[1,4]*Spain*
[2]*USA*
[3]*México*

1. Introduction

The word *pelagic* comes from the Greek πέλαγος meaning *open sea* and refers to the marine and oceanic domain away from the shore line and from surface to bottom (Wikipedia). The *pelagic ecosystem* includes the ever-moving and continuously changing waters, the *habitat*, and the diverse and inter-related groups of organisms or *communities*. Hydrodynamics, forced by external, mostly atmospheric processes set the very special physical conditions that, to a great extent, control the functioning of the biological processes. Currents, waves, mixing, turbulence, air/sea exchanges or fertilization are all mechanisms allowing planktonic communities, the most important in terms of biomass and fluxes of matter and energy, to develop and sustain other communities higher up in the trophic chain.

Since the initial times of Oceanography, modelling the marine system has been mainly applied to the behaviour of its physical properties: temperature, salinity, density, circulation. Forces driving the dynamics of the ocean are heat and water fluxes and wind stress at the free surface, friction between water layers and between water and the solid boundaries and inertia related to the rotation of the Earth. The Navier-Stokes momentum equation

$$\frac{Dv}{Dt} = -\frac{1}{\rho}\nabla p - 2\Omega \times v + g + F_r$$

relates the rate of change of velocity (v) to the field of pressure (p), including Coriolis inertia force (2Ω), gravitation (g), and friction (F_r). This equation has been widely used by physical modellers together with the equation of state of seawater relating density (ρ) to temperature

* Corresponding Author

and salinity (heat and water balance). Since density determines the field of pressure, horizontal gradients of pressure are a key variable in dynamic models for the computation of horizontal and vertical velocities. On the other hand, the continuity condition requires that no gains or losses of water or heat take place other than at the open boundaries (evaporation, precipitation).

In the second half of the 20th century, theoretical ecologists began developing the rationale to simulate the behaviour of both freshwater and marine ecosystems. Much of the work carried out by theoretical ecologists has ended up with highly complex pictorial models (**Figure 1**) not always amenable to numerical simulations. However, as early as in 1949, Gordon A. Riley, a biological oceanographer, and Henry Stommel and Dean Bumpus, two physical oceanographers, published a seminal paper on *Quantitative ecology of the plankton of the western North Atlantic* (Riley at al., 1949). On the other hand, Howard T. Odum developed a theory of ecosystems based on electrical analogs (Odum, 1960), at a time when digital computers were still unavailable, carried out simulations by means of electric circuits. Since then, numerous efforts have been carried out in coupling physical and biological models.

Numerical modelling of the ocean ecosystems was initiated, with some degree of success, in the late 1960s with application to relatively closed coastal lagoons and estuaries (Kremer and Nixon, 1978). However, the complexity of natural biological communities could hardly be modelled by means of "deterministic" causal equations and many of the models made use of stochastic relations to obviate the great variability associated to the genetic and ecological diversity (Margalef, 1972).

Fig. 1. Pictorial model of an ecosystem model (from **wordpress**)

One group of ecological models (today called biogeochemical models) were developed to cope with the need to understand the variability of the planktonic system. Based on the principle that biomass is the material basis of the ecosystem and that organisms are made up of carbon requiring, for their growth and development, the availability of nutrients (nitrogen, orthophosphate, orthosilicic acid, etc.) and light to form such biomass (organic matter) of one or more virtual groups of organisms (photosynthetic microalgae, Bacteria, etc.).

Transfer of biomass through the trophic chain by grazing and predation processes was represented by various forms of equations simulating prey-predator (Lotka-Volterra) dynamics (Lotka, 1925; Volterra, 1926). Part of the carbon and nutrients taken up by primary producers are recycled within the system or exported via faecal detritus or dead organisms settling out of the system. In models of the pelagic system, all or some of the state-variables are subject to physical processes, namely advection and diffusion that, in addition, control the fertility of the system (Steele, 1970).

Biogeochemical models may be as simple as the NPZD (nutrient, phytoplankton, zooplankton, detritus) in which the nutrient (usually nitrogen) is not only the rate-controlling factor, together with light, for photosynthetic growth but also the building block of the entire ecosystem, the assumption being that all other variables are controlled by the Redfield ratio (N:P:C) (Redfield et al., 1963). In these models, availability of light and/or nutrient modifies the maximum theoretical growth rate of the phytoplankton population (nutrient uptake) and both of them modify the density of this population and that of herbivorous, thus controlling the transfer of nutrients from one trophic level to the next. Part of the biomass transferred to the grazing zooplankton is used for the growth of its population while part is excreted back as nutrient to the water or goes into the detritus thus closing the system (Cruzado, 1982; Wroblewski et al., 1988; Wroblewski, 1989; Fasham et al., 1990; Varela et al., 1992, 1994; Bahamon and Cruzado, 2003).

All-inclusive biogeochemical models consider carbon as the building block, with light and various forms of nitrogen (nitrate, ammonia), orthophosphate, silicic acid, iron, etc. controlling primary production (Varela et al., 1995). Dissolved oxygen may or may not be included in the processes of photosynthesis and respiration. However, there seems to be a trend away from modelling entire ecosystems, e.g. large food-web models (Baretta et al., 1995).

In future, ecosystem models will continue to be developed which may be used in support of decision-making. New databases and new measurement (observing) tools will contribute this trend. Nevertheless, important questions still remain open and may be answered with a new generation of ecosystem models which will explicitly contain general principles of ecosystem behaviour. Such models shall aim at process reduction and will be derived from an analysis of present knowledge (Ebenhoh, 2000).

Variability in the physical environment at proper time scales increases the biological activities in the model while the estimate of the primary production is a direct consequence of the dynamic environment. Future operational model applications should include the highest possible resolution of the surface forcing fields and, as the next step, the collection of biological observations necessary at the same scales will be considered to verify the model's capabilities (Vichi, 2000).

Ecosystem modelling has made great advances in the last decades during which it progressed from naive mechanistic and process-oriented modelling to data-driven approaches and individual-based models. Large projects that tried to model whole ecosystems have proven to be of limited use and the trend today appears to go towards more modest and perhaps more successful models of limited aspects of the ecosystems (e.g. special events like toxic algal blooms, etc.)

The coupling of hydrodynamic and biogeochemical models in a three-dimensional framework is a key step toward understanding marine systems and management of marine resources. Ecological processes are strongly influenced by the high heterogeneity in both vertical and horizontal hydrodynamic processes that can only be approached by means of high resolution 3-D models. The purpose of this paper is to highlight the main features of several complementary models applied to parts of the Mediterranean Sea resulting in the best available tools for linking observations (in situ and remote) with theory (both hydrodynamics and ecosystems).

2. The NW Mediterranean

The Mediterranean Sea area, roughly located north of 39°N and limited by the mainland to the north, the Balearic islands to the southwest and the islands of Corsica and Sardinia to the east, is usually called NW Mediterranean sea (NW Med) although different names may be given to subareas such as Gulf of Valencia to the west, Catalan Sea and Gulf of Lions, in the central part, and Ligurian Sea to the east (**Figure 2**).

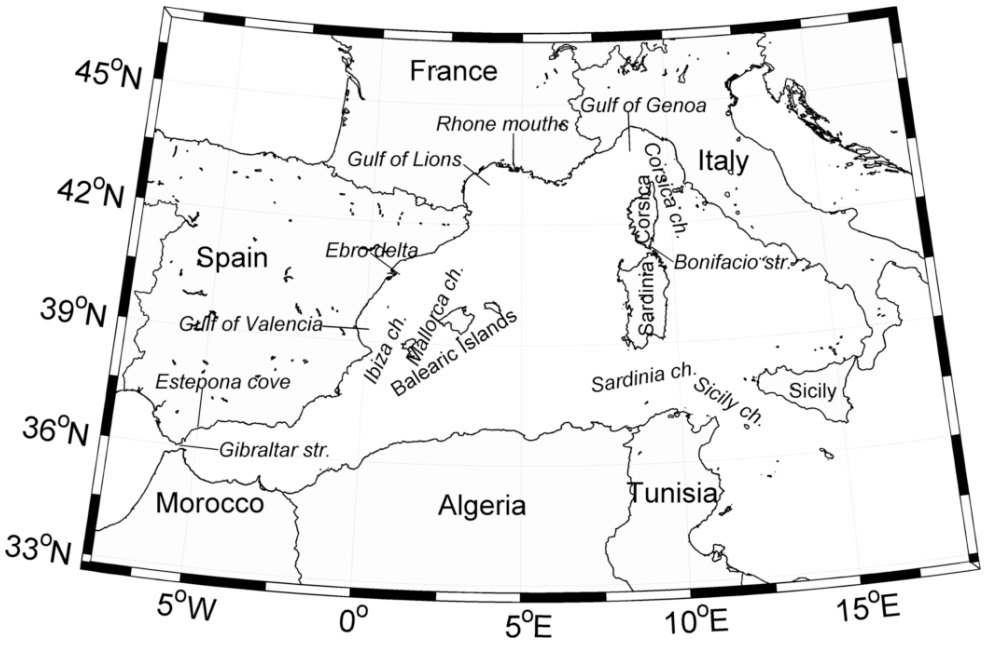

Fig. 2. Map of the Western Mediterranean Sea showing locations cited in this paper.

The NW Med is essentially considered a three layer system: 1) an upper layer between the surface and ~100/200m; 2) an intermediate layer between ~100/200m and ~600/800m; and 3) a deep layer down to the bottom. Three water masses defined mostly on the basis of salinity occupy these layers (**Figure 3**): Modified Atlantic Water, MAW; Levantine Intermediate Water, LIW; and Western Mediterranean Deep Water, WMDW.

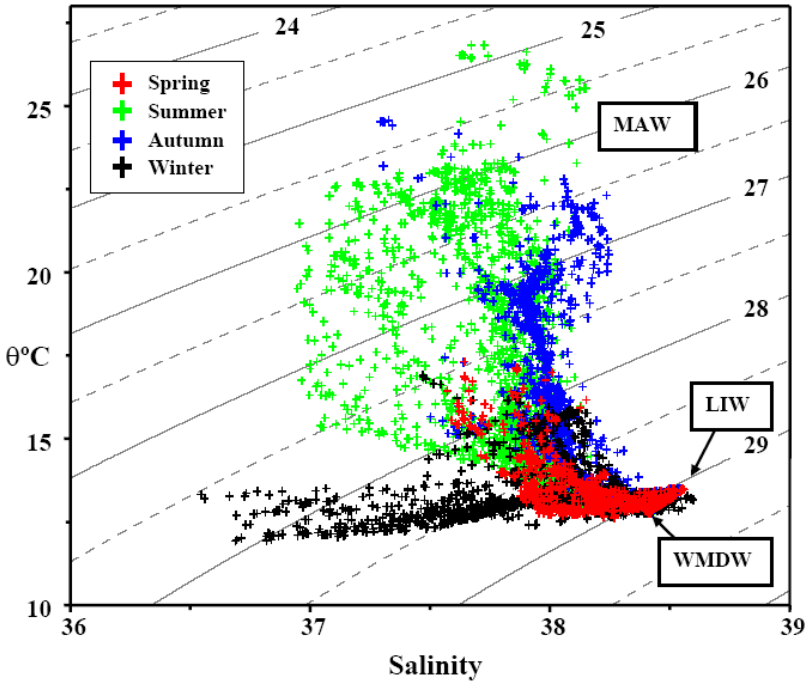

Fig. 3. T-S diagram for the major water masses (MAW, LIW and WMDW) in the NW Mediterranean Sea (Modified from Velasquez, 1997).

Early works pointed out that the major large-scale hydrodynamic feature in the NW Med is a well-defined cyclonic circulation, involving both the MAW surface layer and the LIW layer below (Béthoux et al., 1982). The main component of this circulation is the Northern Current (NC), which is fed by the Eastern and Western Corsican Currents. According to Astraldi et al. (1994), a marked frontal structure found nearly parallel to the coast, separates the Northern Current from the open sea, characterized by a doming of the internal hydrological structure extending from the Ligurian Sea to the Catalan Sea. A general view of the NW Med circulation (**Figure 4**), from large-scale to mesoscale, has been proposed by Millot (1999).

The Ligurian Sea plays an important role for understanding the dynamic characteristics of the whole NW Med (Astraldi and Gasparini, 1992). MAW and LIW enter the sea via northward flows along the east and west coasts of Corsica (Astraldi et al., 1990) converging just north of this island into the Ligurian Current (name given here to the NC). A large-scale cyclonic circulation characterizes the Ligurian Sea, affecting all water masses. The presence

of a thermal front separating the warmer coastal water from those of the interior and a doming of the hydrological structure in the central part of the sea are common features associated to the cyclonic circulation (Crépon and Boukthir, 1987).

The general circulation in the Gulf of Lions, a very complex hydrodynamic area, goes along the continental slope (**Figure 4**). Formation of dense waters both on the shelf and offshore and a seasonal variation of the stratification compete simultaneously in the control of the mesoscale circulation (Millot, 1990).

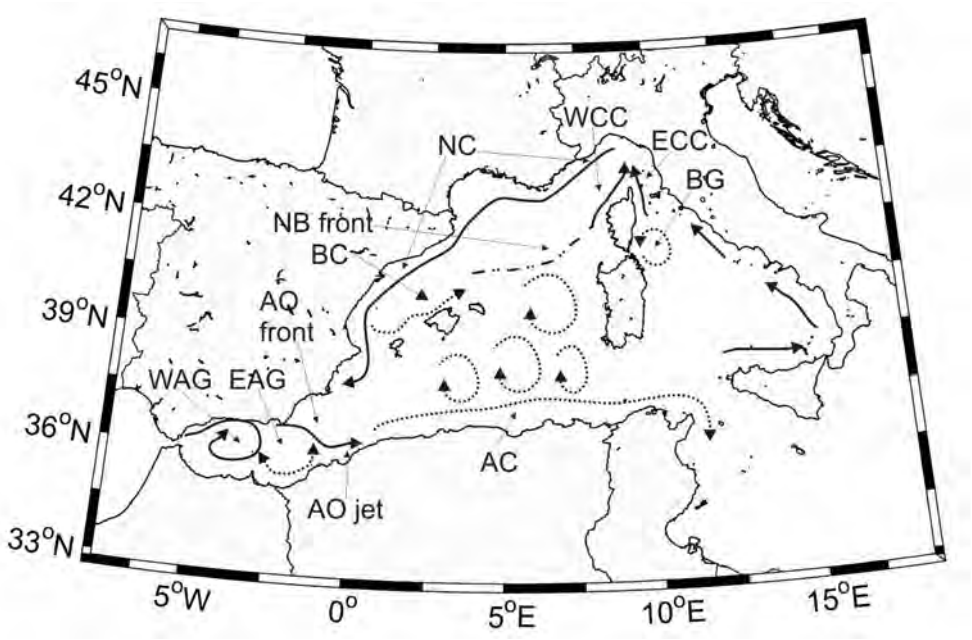

Fig. 4. Major features of the upper layer circulation in the NW Mediterranean Sea (redrawn from Millot, 1999). WAG: Western Alboran Gyre; EAG: Eastern Alboran Gyre; AO jet: Almeria-Oran jet; AC: Algerian Current; AO front: Almeria-Oran front; NB front: North Balearic Front; NC: Northern Current; WCC: Western Corsican Current; ECC: Eastern Corsican Current; BG: Bonifacio Gyre.

During the summer, the Provençal Current (name given here to the NC) flows along the continental slope of the Gulf into the Catalan Sea but, in winter, one part of it deviates from the continental slope off Cap Creus and then follows eastwards. A cyclonic gyre of ~100 km in diameter induces a horizontal divergence at the surface and a convergence at depth, with large vertical motions occurring in the centre (Gascard, 1978). Deep-water formation processes in winter are recognized as a major characteristic of this area (MEDOC Group, 1970; Schott et al., 1996), other significant features being meanders, eddies, "chimneys" and fronts that have also been reported in this part of the NW Med.

The Catalan Sea is a transition zone playing a key role in the general circulation of the NW Med since it connects the two different regimes that configure the Western Mediterranean

dynamics (López-García et al., 1994). The Catalan Sea is characterized by the presence of two permanent density fronts along the continent (the Catalan Front) and along the north slope of the islands (the Balearic Front) and their associated currents. The Catalan Front is a shelf/slope front mainly produced by salinity gradients (Font et al., 1988), that separate the surface layer with denser water in the centre of the sea from the water transported by the Catalan Current (name given here to the NC). In contrast, the Balearic Front is mostly characterized by temperature gradients associated with the so-called Balearic Current (Font et al., 1988; Salat 1995). This front separates the "old" MAW located at the surface in the centre of the Catalan Sea from lighter (and warmer) "recent" MAW flowing northward from the Algerian basin through the Balearic channels. Consequently, the formation of the Balearic Front is determined both by the presence of denser "old" MAW in the centre of the sea and the bottom topography (López-García et al., 1994).

Regarding the biogeochemical properties, the NW Med is known as an oligotrophic environment characterised by high rates of ammonium-based primary production (regenerated production) with relatively scarce contribution from deep water based nitrate (new production) (Dugdale and Goering, 1967). The new to total production (new+regenerated production) ratio (*f*-ratio) in oligotrophic ecosystems is relatively low around 20-30% (*f*-ratio=0.20-0.30) (Eppley and Peterson, 1979). Nevertheless, in temperate zones such as the NW Med, these percentages can strongly vary with seasons. For the summer period with thermal stratification (**Figure 5**), the nutrient shortage in the surface makes the *f*-ratio to be about that expected for oligotrophic ecosystems. However, in winter time, with the breakdown of thermal stratification, nutrient-rich deep waters are brought up to the surface thus providing new nitrogen making the new to total production ratio to increase up to about 0.80 (80%) (Bahamon and Cruzado, 2003).

Phytoplankton (primary) production takes place in the euphotic zone that may show variable thickness with a generally accepted lower limit at the depth of about 3% to 1% the surface irradiance (e.g. Bricaud et al., 1992). At 41° N latitude, the lower limit of the euphotic zone in summer is located at about 50-60 m depth in summer and about 30 m depth in winter (**Figure 5**), as observed at the station OOCS in the Catalan Sea (Bahamon et al., 2011). In the Catalan Sea, the lower limit of the euphotic zone is characterised by a yearly upward nitrogen flux of 0.64 mol N m^{-2} with variations more dependent on the vertical nitrogen gradients than on water density gradients (Bahamon and Cruzado, 2003). This makes the difference with oligotrophic ecosystems at lower latitudes, such as the NE Atlantic Ocean, showing yearly upward nitrogen flux of 0.22 mol N m^{-2}.

The primary production in oligotrophic ecosystems is mostly controlled by nutrient fluxes, PAR availability and zooplankton grazing that has been tested with the use of relatively simple one-dimensional numerical models (e.g. Doney et al, 1996; Bahamon and Cruzado, 2003). In coastal areas of the NW Med, the main fertilization processes fuelling primary production, are the nutrient-rich river water discharges by the Ebro River in the coast of Catalonia and the Rhône River in the Gulf of Lions. In open sea areas, the vertical convection in winter time is the main responsible for fertilising the surface ocean. The central areas of the cyclonic gyres and hydrographic fronts produced by temporary eddies are also responsible for bringing nutrients to the surface from deeper water layers (Estrada, 1995). In the Catalan Sea, despite the spatial chlorophyll variability, coastal and oceanic regions are separated by a distinctive region showing chlorophyll concentration quite

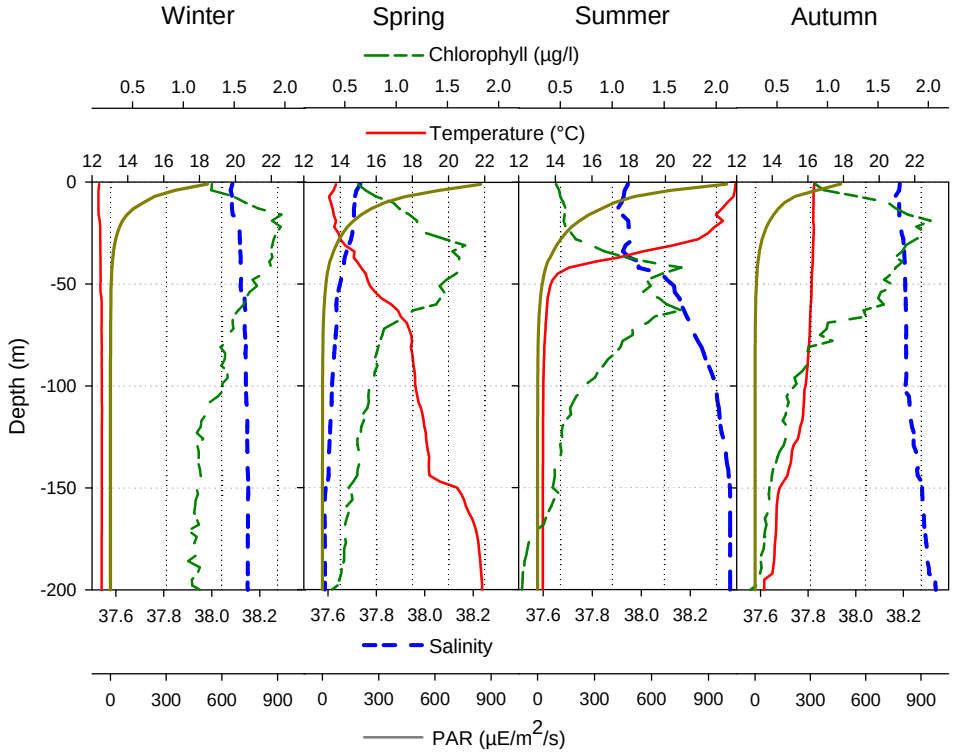

Fig. 5. Average temperature, salinity, PAR and chlorophyll profiles at the station OOCS for the middle of seasons (February, May, August, November) between March 2009 and Feb 2011.

constant throughout the year, following the course for the Northern Current (Gordoa et al., 2008). Although most of surface chlorophyll variability is generally inversely related to temperature this connection is unclear in areas with influence of freshwater discharges (Bahamon et al., 2010; Volpe et al., 2011).

The NW Med shows a subtropical climate with characteristics also found in other areas overseas such as California (USA), central Chile, southern Australia and South Africa (also called Mediterranean climate zones). However, the climate characteristics might be changing in the last decades as suggested by the increasing occurrence of tropical species (Bianchi, 2007) in line with indications of warming of Mediterranean waters (Vargas-Yáñez et al., 2010). In fact, the connection of upper water layers of the pelagic ecosystem to the lower atmosphere allows the strong atmospheric changes recorded in the last years (Vargas-Yáñez et al., 2010; Camuffo et al., 2010) to produce still uncertain effects on the pelagic ecosystem, thus making even more difficult to understand the ecosystem dynamics.

3. Hydrodynamic and biogeochemical modelling rationale

In order to understand and quantitatively describe the functioning of the oceans, physics, chemistry and biology need to be integrated. The fluxes of energy and matter are regulated by the interactions between the physical environment and the elements contained in the waters. The description of the oceanic biogeochemical cycles needs to start from a realistic representation of the oceanic circulation.

We present here results from two hydrodynamic models that represent the three-dimensional circulation on two high-resolution grids (~5 km and ~1.1 km). The first model (WMED) (Bernardello 2010) covers the whole Western Mediterranean Sea, from the Sicilian channel to the straits of Gibraltar. The second model (BLANCA) covers a smaller area in the Catalan Sea centred over the Blanes submarine canyon.

Submarine canyons are irregular steep interruptions of the shelf edge of many continental margins of the world oceans. Because of their interactions with the overlying circulation, submarine canyons are of high biological importance and productivity (Gili et al., 1999; Sardà et al., 2009; Vetter et al., 2010) and often play a significant role on the exchange of energy and matter between the coastal zone and the deep basin (Allen and Durrieu de Madron, 2009).

Since this work is primarily focused on the biogeochemical behaviour of the NW Med and its relationship with the hydrodynamic constraint, we will focus on the surface circulation at basin-scale analysing results from WMED. We will discuss then the circulation within and in the vicinity of the Blanes Canyon as well as the interaction between the incident along-slope flow and the canyon bottom topography using results from BLANCA.

4. The 3D hydrodynamic model

In this work, the codes sbPOM (Stony Brook Parallel Ocean Model) and POM2k are used to simulate hydrodynamics in the NW Med. The models are based on the Princeton Ocean Model (POM). The sbPOM works on a parallelized configuration while POM2k makes use of a single CPU. POM is a finite difference, primitive equations ocean circulation model whose principal attributes, according to Mellor (2004), are: 1) it contains a second order momentum turbulence closure sub-model to provide vertical mixing coefficients; 2) it is a sigma-coordinate model; 3) the horizontal grid uses curvilinear orthogonal coordinates and an "Arakawa C" differencing scheme; 4) the horizontal time differencing is explicit whereas the vertical differencing is implicit; and 5) it has a free surface and a split time step.

In POM, the surface elevation, temperature, salinity, and velocity fields are prognosticated assuming as fundamental hypotheses: 1) the seawater is incompressible; 2) the pressure at any point of the ocean is equal to the weight of the column of water and air above it (hydrostatic approximation); and 3) the density can be expressed in terms of a mean value and a small fluctuation (Boussinesq approximation).

a. Grid set-up, initial and lateral open boundary conditions

The sbPOM was configured for the whole Western Mediterranean (WMED) while POM2k was configured for the North-western Mediterranean (NMS) and for the Blanes Canyon area (BLANCA). The models WMED (resolution of 1/20° in the horizontal and 52 sigma layers in

the vertical) and NMS (resolution of 1/20° in the horizontal and 32 sigma layers in the vertical) get initial and lateral open boundary conditions (salinity, temperature, and velocity) from an operational basin-scale model of the Mediterranean Sea (MFS1671) based on the Océan PArallélisé (OPA) code, which has been configured with a resolution of 1/16° in the horizontal and 72 unevenly distributed z-level layers in the vertical. All the models are run with atmospheric forcing from the European Centre for Medium-Range Weather Forecasts (ECMWF) and ocean (http://www.ecmwf.int/research/era/do/get/era-interim) data assimilation (for more details see Tonani et al., 2008, 2009; Pinardi and Coppini, 2010). The BLANCA model (resolution of 1/60° in the horizontal and 32 sigma layers in the vertical) in particular gets initial and lateral open boundary conditions from the NMS outputs. The WMED model was run for the period 2001-2008 and the NMS and BLANCA models were run for the year 2001.

The WMED model has two lateral open boundaries at the strait of Gibraltar and the Sicilian channel, the NMS model has one lateral open boundary at 40°N and the BLANCA model has two lateral open boundaries at 41° 18.6′N and 3° 6.0′E. The first two models are fed with salinity, temperature, and velocity fields from MFS outputs. Given that WMED and NMS have different horizontal resolution than MFS, a horizontal bilinear interpolation was necessary. Since the vertical coordinate system is also different, MFS outputs were transformed from z-levels to sigma layers using a linear interpolation. The BLANCA, on the other hand, is fed with salinity, temperature and velocity fields from NMS outputs.

Since BLANCA has different horizontal resolution than NMS, a horizontal bilinear interpolation was necessary while, in the vertical, the grid is not refined as both models have the same number (32) of vertical layers. Furthermore, in order to avoid inaccuracies in the interpolation, which can generate errors leading to distortions of the model solution at the lateral open boundary or to violation of mass conservation, a volume conservation constraint [Marchesiello et al., 2001; Korres and Lascaratos, 2003; Sorgente et al., 2003; Zavatarelli and Pinardi, 2003] was imposed on the interpolated normal velocity across the lateral open boundaries thus guaranteeing volume conservation between MFS and WMED, between MFS and NMS and between NMS and BLANCA. Finally, to avoid temporal discontinuities at the lateral open boundaries, salinity, temperature, and velocity were specified at each time step using a linear interpolation in time between consecutive fields.

b. Mean dynamic topography and geostrophic circulation in the Western Mediterranean Sea from WMED model outputs

The mean dynamic topography (MDT) is the sea elevation due to the mean oceanic circulation. The only MDT available for the Mediterranean Sea was reconstructed combining oceanic observations as altimetry and in-situ measurements and outputs from an ocean general circulation model with no data assimilation for the period 1993-1999 (Rio et al., 2007). This MDT (hereafter called RioMDT) and the associated geostrophic circulation are compared to those estimated by the WMED model (**Figure 6**).

The NW Med is characterized by a mean cyclonic circulation whose northern side corresponds to the Northern current (NC; Millot, 1999). In the RioMDT the NC is clearly visible along the northern coast from Italy up to the Ibiza channel while in the model MDT it appears somewhat more intense on the Italian coast and, then, starts decreasing along the Spanish coast where it appears weak and hardly noticeable at the level of the Ibiza channel.

The progression of the NC southwestwards is characterized by a weakened flow and increased variability caused by complex interactions with incoming southern waters near the Balearic Islands (Garcia-Ladona et al., 1994). From current measurements performed 35 Km off the Ebro delta, Font et al. (1995) reported a mean speed of the order of 5 cm s^{-1}. The RioMDT shows high speed values (~35 cm s^{-1}) even south of the Ebro delta while the model MDT shows low values and the mean flow is not well defined. The general pattern obtained by Font et al., (1988) from climatological studies, describes the bifurcation of the NC at the height of the Ibiza channel. One branch of the current would then cross the channel transporting water southwards in the Algerian Basin becoming older Mediterranean water while the other branch returns cyclonically to the northeast forming the Balearic current (BC).

Garcia-Ladona et al., (1996) described the BC as formed by an incoming flux of Mediterranean Atlantic Water (MAW) through the Ibiza channel and the recirculation of old MAW from the NC. This description seems to agree with both MDT. In the RioMDT the BC seems to be fed by both the deflection of the NC and new MAW entering through the Ibiza channel. In the model MDT, the latter factor seems to be determinant for the existence of the current up to the island of Mallorca, where the eastward deflection of the NC strengthens the flow towards the center of the Algero-provençal Basin (**Figure 6**).

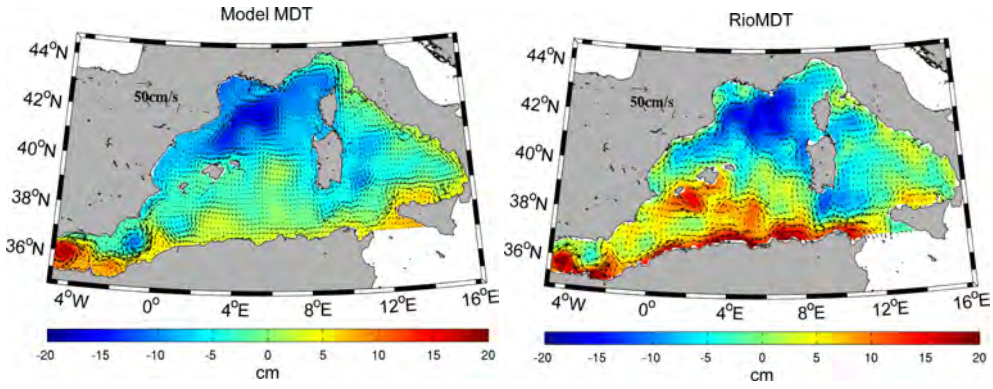

Fig. 6. Model MDT and RioMDT with associated geostrophic currents

Despite the uncertainty regarding the variability of the flux, specially in the Ibiza channel (Astraldi et al., 1999), the Balearic channels are commonly accepted to be the way through which MAW is transported to maintain the Balearic density front. This front is associated to the BC and has been described as a salinity front (Lopez-Garcia et al., 1994; Garcia-Ladona et al., 1996). The overall averages of model surface salinity and temperature are shown with the geostrophic currents superposed in **Figure 7**. The model reproduces the wavelike shape of the salinity front and the geostrophic current associated on the northern side of Mallorca, as described by La Violette et al. (1990).

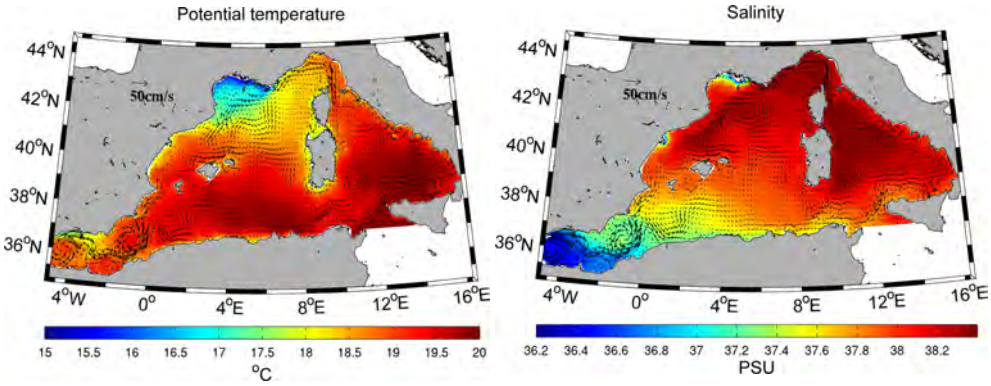

Fig. 7. Mean sea surface temperature and salinity for the whole simulation period. Geostrophic currents associated to model MDT are superposed

The NC is also associated to a permanent horizontal density gradient called the Catalan front. This front is maintained by a cool plume of water flowing along the Iberian Peninsula and originated in the Gulf of Lions (La Violette et al., 1990) or by low salinity due to the continental runoff (Font et al., 1988) or both (Garcia-Ladona et al., 1996). The model reproduces the Catalan front in both salinity and temperature, the latter being more pronounced (**Figure 7**).

c. The circulation within and around the Blanes submarine canyon from BLANCA outputs

Month	N (s^{-1})	R_d (km)	T_r (m)	Ro
January	0.0018	18.55	209.4	0.44
February	0.0015	15.46	253.7	0.47
March	0.0015	15.46	244.0	0.49
April	0.0018	18.55	206.3	0.44
May	0.0021	21.64	182.1	0.40
June	0.0026	26.80	144.3	0.44
July	0.0027	27.83	139.7	0.47
August	0.0028	28.86	135.0	0.41
September	0.0031	31.95	120.7	0.36
October	0.0032	32.98	119.7	0.40
November	0.0029	29.89	130.5	0.51
December	0.0022	22.68	169.2	0.50

N is the mean buoyancy frequency ($[-g/\rho_0\,(\Delta\rho/\Delta z)]^{1/2}$), $\mathbf{R_d}$ is the internal Rossby radius of deformation (NH/f), $\mathbf{T_r}$ is the vertical stratification scale (fL/N) and **Ro** is the Rossby number (U/fL). **H** is the canyon depth at the mouth= 1000m, $f = 2\Omega\sin\varphi$, $\Omega = 7.292\text{x}10^{-5}$ rad s^{-1}, φ=41.363°N, $\mathbf{f} = 9.7\text{x}10^{-5}$ s^{-1}, **W** is the canyon width at the mid-upper canyon= 8.0km, $\mathbf{L}=W/2$= 4km, $\mathbf{H_s}$ is the shelf-break depth=150m (Flexas et al., 2008).

Table 1. Variability of hydrodynamic properties for the Blanes submarine canyon

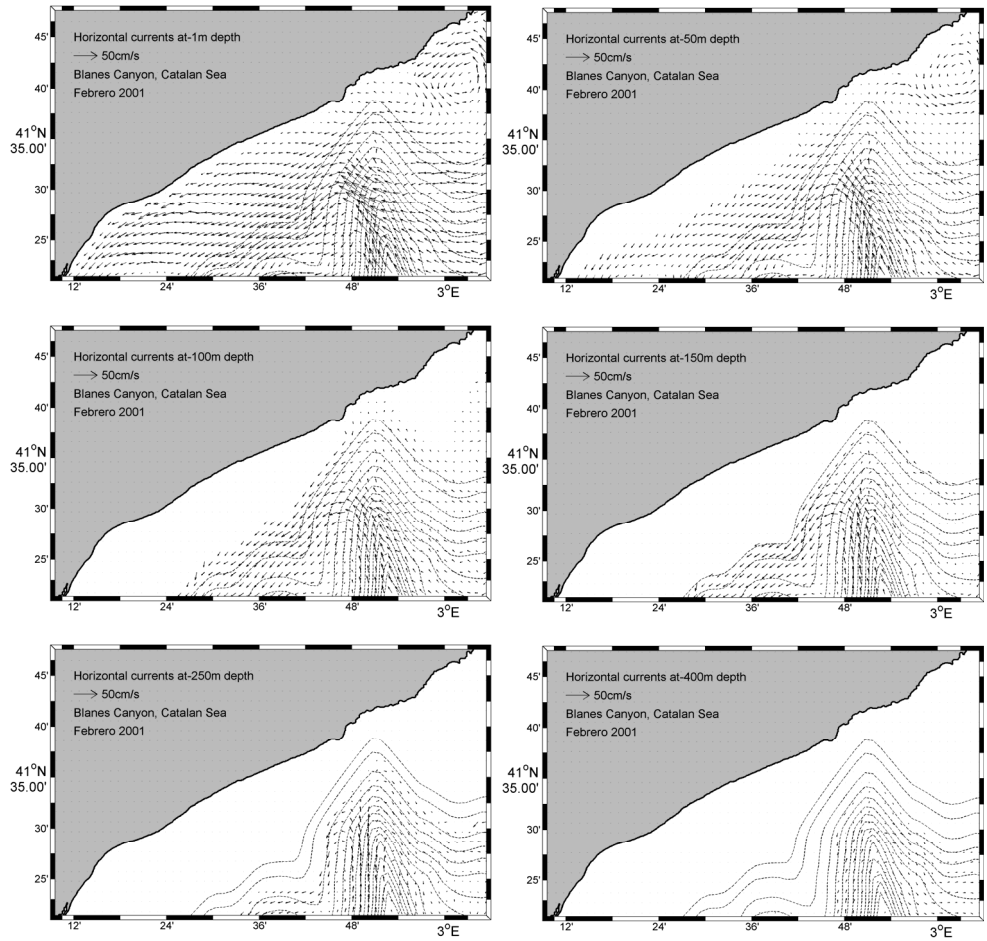

Fig. 8. Surface velocity at 1, 50, 100, 150, 250 and 400 m depth simulated with the BLANCA model

Since this section is mainly on the circulation within and in the vicinity of the Blanes submarine canyon, we will focus on analysing the BLANCA model results. In order to do this, the water column stratification and some dynamical considerations are presented (**Table 1**). On the other hand, horizontal velocity fields at different depths (1, 50, 100, 150, 250, and 400m) are used to provide an analysis of the circulation during a mid-winter month (February) characterized by moderate NW winds, net heat loss through the sea surface and weak stratification of the water column (**Figure 8**).

The seasonal variation of the water column stratification in the Blanes canyon is confirmed. Strongest stratification is displayed in September (N=0.0031s-1) and October (N=0.0032s-1) when the sea surface begins to lose heat and wind is still relatively weak. During November

(N=0.0029s-1), after strong wind bursts, stratification begins to be eroded. From December to March (N=0.0022-0.0015s-1), under the effects of strong wind and progressive cooling of the sea surface, stratification becomes increasingly weaker. Finally, from April to August (N=0.0018-0.0028s-1), as wind weakens and the sea surface gains heat, stratification becomes progressively stronger. In summary, stratification increases from April to October and decreases from November to March (Table 1, column 2).

Before examining the circulation within the Blanes canyon, it is important to review the relevant scales of motion. In this context, a key parameter for the resulting interactions between canyon topography and the incident flow is the ratio of the canyon width (W) to the local internal radius of deformation (Rd). A submarine canyon is considered narrow when it is narrower than half the smallest local internal radius of deformation (i.e. W<Rd/2) (Klinck, 1988; 1989). If a canyon is narrow, then cross-canyon geostrophic flow is inhibited, while along-canyon ageostrophic flow caused by the unbalanced pressure gradients would create substantial cross-shelf exchange. In contrast, if a canyon is wide, a geostrophic balance can be reached within the canyon, resulting in a cross-canyon flow, that is, the canyon merely steers the flow around the isobaths and so the horizontal pressure gradient remains balanced and no up- or downwelling occurs (Klinck, 1988; 1989; 1996; Hickey, 1995; Chen and Allen, 1996; Garcia-LaFuente et al., 1999; Jordi et al., 2005; Flexas et al., 2008; Allen and Durrieu de Madron, 2009).

According to the above-mentioned criterion, the Blanes canyon is moderately narrow, that is, the canyon width (~8 km) is slightly more than half the smallest local internal radius of deformation (15.46 km; Table 1, column 3). It is also deep, that is, the depth of the canyon below its rim is approximately three times the depth of the simulated incident flow (~1000 m versus ~300 m). On the other hand, the vertical stratification scale (Tr), that provides the distance above the canyon in which the flow will remain unaffected by the presence of the canyon (Craig, 2006; Flexas et al., 2008), exhibits values between ~119 m and ~253 m for strong and weak stratification conditions respectively (Table 1, column 4). Furthermore, an indicator of nonlinearity within a submarine canyon is the Rossby number (Ro) representing the relative importance of momentum advection (Klinck, 1996; Hickey, 1997; Skliris et al., 2001; Allen and Durrieu de Madron, 2009). For the simulated incident flow, which displays velocities between ~10 and 15 cm $\cdot s^{-1}$ at the shelf-break, Ro ranges from 0.36 to 0.51 (Table 1, column 5) indicating that momentum advection plays an important role on the flow pattern.

In mid-winter, the Blanes canyon topographic effects on the incident flow field are clearly observed from the sea surface to the bottom (**Figure 8**). Above the canyon rim (i.e. from the sea surface down to 100 m depth), the NC entering the canyon is deflected toward the coast at the same time that the increase of the depth gradient leads to an increase in the current velocity (maximum daily-averaged current speeds near the canyon axis of about 35, 30 and 20 cm $\cdot s^{-1}$ at 1 m, 50 m and 100 m depth respectively). While the onshore edge of the NC flows toward the west wall of the canyon head crossing the canyon isobaths, the offshore edge flows toward the upper canyon across them. Passing the canyon axis, the NC is again deflected and flows south-westward crossing the isobaths of the west wall of the canyon.

Over the shelf, there is also a south-westward flow with maximum daily-averaged near-surface (at 1 m depth) current speeds of about 25-30 cm·s^{-1}. The overall pathway and the offshore intensification of this current suggest a possible link with the local dynamics of the NC resulting from its interaction with the canyon topography. Further north-east, over the north-easternmost inner shelf, there is a cyclonic gyre characterized by maximum daily-averaged near-surface current speeds of about 20-25 cm·s^{-1}. At 150 m depth (i.e. below the canyon rim), the circulation patterns are very similar to those observed in the upper layers. The NC is also deflected toward the coast over the east wall of the canyon and then, passing the canyon axis, it is steered south-westward.

The main difference with the upper circulation patterns is a weak anticyclonic circulation (daily-averaged current speeds less than 15 cm·s^{-1}) observed over the east wall of the upper canyon. These circulation patterns are rather different at 250 m. At this depth, a dipole-like structure with anticyclonic (cyclonic) circulation over the east (west) wall of the canyon is observed. In this structure, the divergence zone is located on the western side of the canyon axis. At greater depths (i.e. from 400 m depth down to the bottom), the flow steered by the canyon topography tends to follow along the canyon walls describing an anticyclonic path with a maximum daily-averaged current speed ranging 8 to 10 cm·s^{-1}.

5. The 3D biogeochemical model

The appropriate basis for the study of marine biogeochemical cycles is the coupling of models that integrate physical, chemical and biological processes. In this section we present results from the biogeochemical component of WMED over the period 2001-2008.

The quantitative assessment of the predictive capability of a model is necessary before it is used with any degree of confidence for either scientific or operational purposes (Holt et al., 2005). Validating three-dimensional models is difficult because of the general paucity of observational data at the proper spatial and temporal scales (Lehmann et al., 2009). In this context, satellite imagery is a valuable data source because of its synopticity over wide areas.

Weekly composite images of chlorophyll (Chl) for the Western Mediterranean are detailed enough to fill most of the gaps caused by cloud cover. The resulting data set is robust and can be used for objective validation of model outputs. Quantitative metrics that measure the agreement between model predictions and observational data have recently received increasing attention (Allen et al., 2007). Remotely sensed chlorophyll was used for this purpose by Lacroix et al., (2007) in the North Sea and by Lehmann et al., (2009) in the western North Atlantic Ocean. Some of these metrics are used here to perform a quantitative validation of the model skill as a predictor of surface variability.

The biogeochemical model developed for this study is an aggregated-type model based on previous developments by Cruzado (1982), Fasham et al. (1990), Varela et al. (1992) and Bahamon and Cruzado (2003). It consists of different compartments representing nitrate, ammonium, phytoplankton, bacteria, zooplankton, detritic matter and dissolved organic matter and uses nitrogen as currency. Nitrogen fluxes among these compartments are parameterized in order to describe the main biogeochemical processes occurring at the lowest levels of the marine pelagic food-web (**Figure 9**).

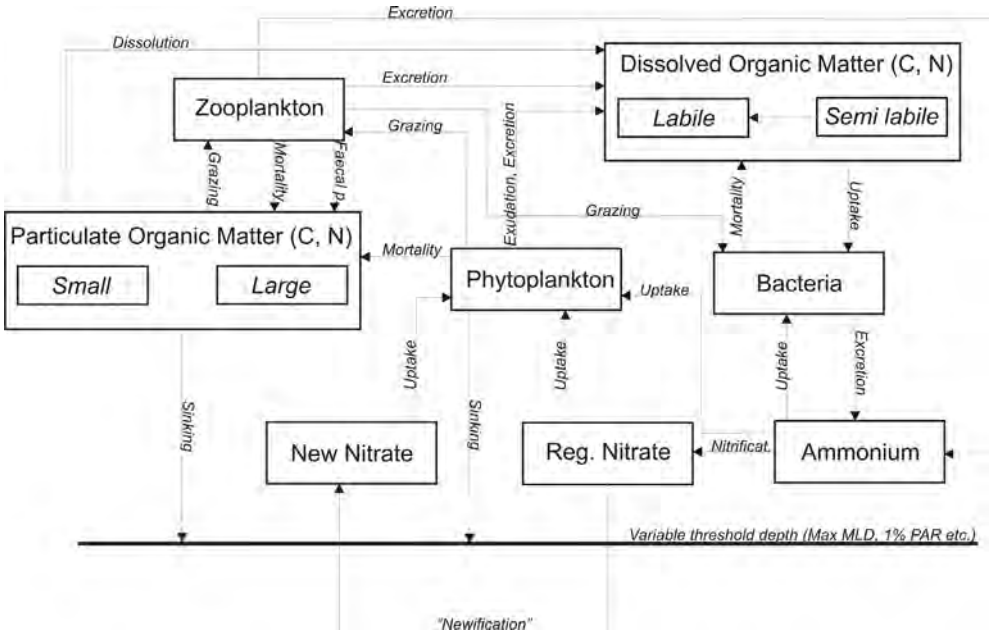

Fig. 9. Biogeochemical model description. Boxes show compartments and arrows correspond to fluxes.

Nitrogen is a key element for understanding the nutrient flow in the Mediterranean because its fractionation covers different aspects of processes occurring in the ecosystem (Dugdale and Wilkerson, 1988). Mediterranean waters show a general deficiency of phosphorus with respect to the world ocean with high N:P ratios (about 20-23). Several studies in the Western Mediterranean have pointed to phosphorus as an important limiting nutrient for phytoplankton growth (Thingstad et al., 1998; Diaz et al., 2001). Nevertheless, other scientists proved nitrogen to be the main limiting factor in the photic zone, phosphorus being potentially limiting only when other factors (light or nitrogen) are limiting at the same time (Bahamon and Cruzado, 2003; Lucea et al., 2003; Leblanc et al., 2003).

Compartments were introduced to better represent the vertical flux of particulate and dissolved organic matter. Particulate matter was split into small and large detritus and dissolved organic matter into labile and semi-labile fractions. Some degree of complexity was allowed by considering variable C:N ratios of decaying matter (both detritus and dissolved organic matter). The phytoplankton and zooplankton compartments include all the autotrophic and heterotrophic pelagic organisms without any functional or dimensional distinction. The number of state variables has been set to fourteen, ten for nitrogen and four for carbon. This configuration allows closing the cycle of nitrogen in a mass-conservative way while the cycle of carbon is only partially described and its total mass is not conserved. In fact, dissolved inorganic carbon is not considered as a state variable and this is equivalent to assume that it never limits primary production.

a. Statistics of model/observation fit

Level 3 weekly composite maps from sensor Aqua-MODIS were downloaded from NASA Ocean Colour Home Page. The images were interpolated to the model grid obtaining a data series that spans from June 2002 to December 2008. Four statistics frequently used to quantify agreement between model (*M)* and observations (*O*) are calculated for Chl: model bias (*Bias*), root mean square error (*RMSE*), model efficiency (*ME*) and correlation coefficient (*CRC*). In the following equations the total number of model/observation data pairs is indicated as *n* and summations are performed over the time dimension. Bi-dimensional maps are obtained for each index. The average over time allows visualizing spatially explicit error statistics that quantify the temporal agreement between model and observations at the spatial resolution of the model. This is useful in highlighting regional differences in the performance of the model.

The model bias represents the mean deviation between model estimates and observations. It provides a measure of whether the model is systematically underestimating (*Bias*<0) or overestimating (*Bias*>0) the observations. Note that *Bias* is able to reveal only a persistent error in magnitude of the modelled variable because negative and positive deviations tend to cancel each other in the summation.

$$Bias = \frac{1}{n}\sum(M - O)$$

Root mean square error (*RMSE*) measures the misfit between model and observations by neutralizing the sign of the deviation:

$$RMSE = \sqrt{\frac{\sum(M - O)^2}{n}}$$

Negative and positive contributions are added; then the square-root restores the unit to that of the variable considered.

Model efficiency (*ME*) is the proportion of the initial variance accounted for by the model:

$$ME = 1 - \frac{\sum(M - O)^2}{\sum(O - \overline{O})^2}$$

ME gives the deviation of the predicted values from the observed values in relation to the scattering of the latter. The maximum value for this indicator is 1 which corresponds to an explained variance of 100%. The over-bar denotes the average over *n*.

The correlation coefficient (*CRC*) indicates the quality and direction of a linear relationship between two variables:

$$CRC = \frac{\sum\left(O - \overline{O}\right)\left(M - \overline{M}\right)}{\sqrt{\sum(O - \overline{O})^2 \sum(M - \overline{O})^2}}$$

b. Chlorophyll validation

The surface averages of model and MODIS chlorophyll for the whole time-series are shown in **Figure 10**. The overall agreement is reasonable as the model reproduces well the seasonal cycle with a good timing for the spring bloom and the summer oligotrophy. In late summer and autumn the model tends to overestimate the surface chlorophyll concentrations specially during 2003 and 2004 when the model simulates a secondary autumn peak not visible in the MODIS series. From autumn to winter the decrease in chlorophyll concentration in the MODIS series is hardly noticeable while in the model seems to be a recurrent feature causing the winter underestimation of chlorophyll. The interannual variability seems to be restricted to the duration and intensity of the spring bloom and is well captured by the model.

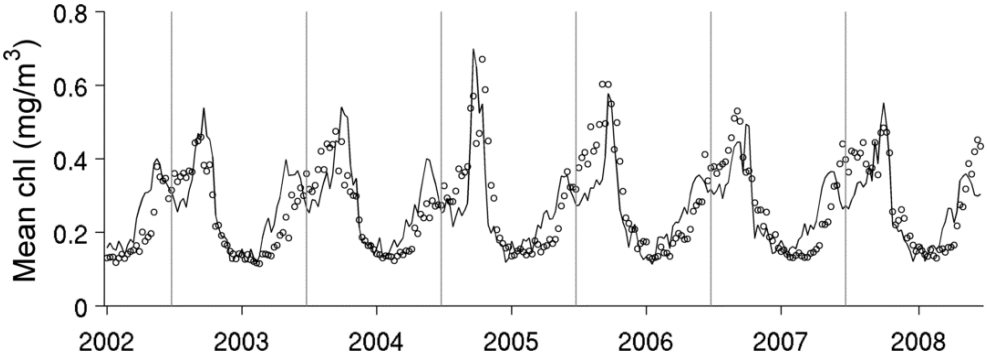

Fig. 10. Area-averaged chlorophyll for MODIS (circles) and model (continuous line). R=0.79, p< 0.01

The spatially resolved statistic indexes of the fit between model and MODIS chlorophyll are shown in **Figure 11**. The bias shows a general model underestimation along the coast in the Gulf of Lions, the Gulf of Valencia, the western Alboran Sea and along the Italian coast. It should be recalled that, in coastal areas, remotely sensed surface chlorophyll is likely to be overestimated due to the presence of inorganic sediments and coloured dissolved organic matter. This is certainly the case for the Gulf of Lions and the northern part of the gulf of Valencia where continental freshwater inputs are important. The Rhône and the Ebro rivers are the most important effluents in the NW Med and, though their influence is taken into account by the model as total nitrogen input, the inorganic sediment load can significantly complicate the interpretation of the colour signal. The same happens along the Italian coast where a certain number of smaller rivers (Liri-Garigliano, Tevere, Arno, Magra etc.) can bring considerable amount of sediments to the coastal waters.

In seasonal composite maps of remote sensing chlorophyll, the northern part of the western Mediterranean Sea is characterized by the presence of an area with concentrations higher than in the southern part. This is true during spring, summer and autumn while during winter the picture is opposite. This area interests the Gulf of Genova up to the Balearic Sea and is limited on the southern edge by the presence of islands (Corsica and Balearic) at its longitudinal extremes while in the centre, in front of the Gulf of Lions, the southern limit

roughly coincides with the North-Balearic (NB) front. This area is enclosed by the general cyclonic circuit formed by the Northern Current (NC), the Balearic Current (BC), the NB front and the Western Corsican Current (WCC). Furthermore, it is an important site of deep water formation, specially in its central part.

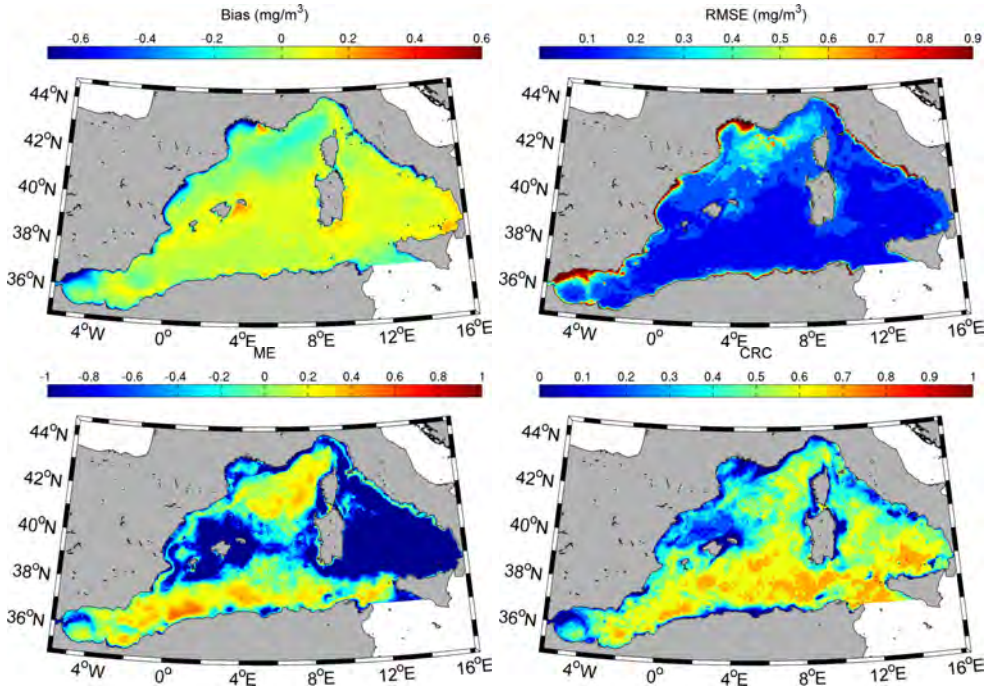

Fig. 11. Spatial distribution of Bias, RMSE, ME and CRC

This means that the vertical dynamics are particularly energetic during winter determining at the same time a dramatic nutrient replenishment of the euphotic zone and a reduction of light exposure for phytoplankton. This explains the so-called ``blue holes'' that correspond to reduced chlorophyll concentrations during winter (Barale et al., 2008).

With the progression of winter, the wind forcing decreases leading to the stabilization of the water column what results in the start of the spring bloom. Once the spring bloom has exhausted the surface nutrients, oligotrophic conditions prevail with the onset of summer stratification. During summer, the cyclonic-induced doming of the isopycnals and of the nutricline is still able to determine an enhancement of the nutrient flux into the euphotic zone. This flux is reduced by the thermal stratification but is sufficient to determine the presence of higher chlorophyll concentrations with respect to the surrounding areas. The area of higher chlorophyll is now narrower and reduced to its north-eastern part from the Gulf of Lions to the Gulf of Genova. The *Bias* for chlorophyll concentration shows model underestimation over an area that roughly coincides with the summer chlorophyll distribution. The shape and extension of the area is confirmed by *RMSE* while both *ME* and *CRC* point to a good performance of the model. This means that the underestimation of

chlorophyll by the model is probably restricted to summer being the signal of the spring bloom determinant to obtain good results for *ME* and *CRC*.

6. Summary and conclusions

The three-dimensional modelling of hydrodynamic and biogeochemical processes taking place in the NW Med pelagic ecosystem (WMED and BLANCA models) presented here compare to in-situ and remote sensing observations. This is achieved because the models simulate key physical processes shaping the hydrodynamics over the Western Mediterranean basin and sub-basins (WMED model) and in a coastal area (mesoscale) strongly influenced by the submarine Blanes canyon bathymetry (BLANCA). The WMED model also allowed a satisfactory representation of the biogeochemical processes (e.g. heat transport, momentum and biogeochemical tracers) conducting the seasonal fluctuations of phytoplankton primary production.

Modelling the oligotrophic pelagic ecosystem dynamics is suitable for understanding and quantifying relatively complex processes related to energy and matter transfer constrained by advective and diffusive processes. Although not developed with all limiting nutrients for phytoplankton growth, e.g. the biogeochemical model assessed nitrogen-based matter fluxes, it allows explaining the primary production based on diffusivity and advection processes through the water column and based on the mixing produced by winter convection fuelling the phytoplankton bloom in late spring.

Both models are excellent tools for the study of past and future evolution of the physical and biogeochemical environment in an area that is subject to important anthropogenic pressures (navigation, fishing, tourism, industry, agriculture, coastal development, etc.). Robust tools such as these are crucial for assessing the impact exerted up to the present or expected to be made in future. Marine ecosystem analysis and operational oceanography are two scientific and technical fields in which combined disciplines are key for their success. On the other hand, observations by means of satellites or autonomous moored or drifting sensors are also crucial to validate models making them indispensable in the forecasting of future scenarios.

7. References

Allen, J.I., Somerfeld, P.J. and Gilbert, F.J. (2007). Quantifying uncertainty in high-resolution coupled hydrodynamic-ecosystem models. *Journal of Marine Systems* 64(1-4): 3 - 14.

Allen S.E. and Durrieu de Madron, X. (2009). A review of the role of submarine canyons in deep-ocean exchange with the shelf. *Ocean Science* 5: 607-620.

Astraldi, M., Gasparini, G.P. and Manzella, G.M.R. (1990). Temporal variability of currents in the Eastern Ligurian Sea. *Journal of Geophysical Research* 95(C2):1515-1522.

Astraldi M. and Gasparini, G.P. (1992). The seasonal characteristics of the circulation in the North Mediterranean Basin and their relationship with the Atmospheric-Climate Conditions. *Journal of Geophysical Research* 97(C6): 9531-9540.

Astraldi, M., Gasparini, G.P. and Sparnocchia, S. (1994). The seasonal and interannual variability in the Ligurian-Provencal Basin. *Coastal and Estuaries Studies* 46:93-113.

Astraldi, M., Balopoulos, S., Candela, J., Font, J., Gacic, M., Gasparini, G.P., Manca, B., Theocharis, A. and Tintore, J. (1999). The role of straits and channels in understanding the characteristics of Mediterranean circulation. *Progress in Oceanography* 44(1-3): 65-108. ISSN0079-6611.

Bahamon, N. and Cruzado, A. (2003). Modelling nitrogen uxes in oligotrophic environments: NW Mediterranean and NE Atlantic. *Ecological Modelling* 163(3): 223-244. ISSN 0304-3800

Bahamon, N., Cruzado, A., Velasquez, Z., Bernardello, R. and Donis, D. (2010). Patterns of phytoplankton chlorophyll variability in Mediterranean Seas. Rapp. *Comm. int. Mer Médit*. 39: 436.

Bahamon, N., Aguzzi, J., Bernardello, R., Ahumada-Sempoal, M-A., Puigdefabregas, J., Cateura, J., Muñoz, E., Velásquez, Z. and Cruzado, A. (2011). The new pelagic Operational Observatory of the Catalan Sea (OOCS) for the multisensor coordinated measurement of atmospheric and oceanographic conditions. *Sensors* 11: 11251-11272.

Barale, V., Jaquet, J.-M. and Ndiaye, M. (2008). Algal blooming patterns and anomalies in the Mediterranean Sea as derived from the SeaWiFS data set (1998-2003). *Remote Sensing of En- vironment*: 112(8), 3300 - 3313. ISSN 0034-4257.

Baretta, J.W., Ebenhöh, W. and Ruardij, P. (1995): The european regional seas ecosystem model, a complex marine ecosystem model. *Netherlands Journal of Sea Research* 33(3/4), 233-246.

Bethoux, J.P., Prieur, L. and Nyffeler, F. (1982). The water circulation in the North-western Mediterranean Sea, its relations with wind and atmospheric pressure. Hydrodynamics of semi-enclosed seas. Proceeding of the 13th International Liege Colloquium on Ocean Hydrodynamics. J.C.J., Nihoul (editor). *Elsevier Oceanography Series* 34:129-142.

Bianchi, C.N. (2007). Biodiversity issues for the forthcoming tropical Mediterranean Sea. *Hydrobiologia* 580:7–21.

Bricaud, A., Morel, A. and Tailliez, D. (1992). Mesures optiques. In: Neveux, J. (Ed.), Les maximums profonds de chl a en mer des Sargasses. Donnees physiques, chimiques et biologiques. Campagne Chlomax. Campagnes Oceanographiques.

Camuffo, D., Bertolin, C., Diodato, N., Barriendos, M., Dominguez-Castro, F., Cocheo, C., della Valle, A., Garnier, E., and Alcoforado, M. (2010). The western Mediterranean climate: How will it respond to global warming? *Climatic Change* 100:137-142.

Chen, X. and Allen, S.E. (1996). The influence of canyons on shelf currents: A theoretical study. *J. Geophysical Research* 101(C8): 18043-18059.

Craig, W. A. (2006). The Flinders Current and Upwelling in Submarine Canyons. *Master Thesis, UNSW*, Australia, 118 pp.

Crépon, M. and Boukthir, M. (1987). Effect of deep water formation on the circulation of the Ligurian Sea. *Annals of Geophysics* 5B (1):43-48.

Cruzado, A. (1982). Simulation model of primary production in coastal upwelling off western sahara. *J. Cons. perm. int. Explor Mer.* 180: 5-6.

Diaz, F., Raimbault, P., Boudjellal, B., Garcia, N. and Moutin, T. (2001). Early spring phosphorus limitation of primary productivity in a NW Mediterranean coastal zone (Gulf of Lions). *Marine Ecology Progress Series* 211: 51–62.

Doney, S.C., Glover, D.M. and Najjar, R.G. (1996). A new coupled, one-dimensional biological–physical model for the upper ocean: applications to the JGOFS Bermuda Atlantic Time-Series Study (BATS) site. *Deep-Sea Research II* 43: 591–62

Dugdale, R.C. and Goering, J.J. (1967). Uptake of new and regenerated forms of nitrogen in primary productivity. *Limnology and Oceanography* 12: 6: 206.

Dugdale, R.C. and Wilkerson, F. P. (1988). Nutrient sources and primary production in the Eastern Mediterranean. *Oceanologica Acta* 11: 179 – 184

Ebenhoh, W. (2000). Critical analysis of the *status quo* in marine ecosystem modeling. Biological Observations in Operational Oceanography. EuroGOOS Publication Nº 15, EuroGOOS Office, Southampton.

Eppley, R. W. and Peterson, B. J. (1979). Particulate organic matter flux and planktonic new production in the deep ocean. *Nature* 282: 677-680.

Estrada, M. (1995). Primary production in NW Mediterranean. *Scientia Marina* 60(Supl.2): 55-64.

Fasham, M.J.R., Ducklow, H.W. and McKelvie, S.M. (1990). A nitrogen-based model of plankton dynamics in the ocean mixed layer. *Journal of Marine Research* 48(3): 591 – 639

Flexas, M.M., Boyer, D.L., Espino, M., Puigdefàbregas, J., Rubio, A. and Company, J.B. (2008). Circulation ovear a submarine canyon in the NW Mediterranean. *Journal of Geophysical Research* 113(C12002), doi: 10.1029/2006JC003998.

Font, J., Salat, J. and Tintore, J. (1988). Permanent features of the circulation in the Catalan Sea. *Oceanologica Acta* 9: 51-57.

Font, J., Garcia-Ladona, E. and Gorriz, E. (1995). The seasonality of mesoscale motion in the Northern Current of the western Mediterranean: several years of evidence. *Oceanologica Acta* 18, 207-219.

Garcia-Ladona, E., Tintore, J., Pinot, J., Font, J. and Manriquez, M. (1994). Surface circulation and dynamics of the Balearic Sea. In La Violette, P., ed., The seasonal and interannual variability of the Western Mediterranean Sea, Coastal and Estuarine Studies, pp. 73-91.

Garcia-Ladona, E., Castellon, A., Font, J. and Tintore, J. (1996). The Balearic current and volume transport in the Balearic basin. *Oceanologica Acta* 19, 489-497.

Garcia-LaFuente, J., Sarhan, T., Vargas, M., Vargas, J.M. and Plaza, F. (1999). Tidal motions and tidally induced fluxes through La Línea submarine canyon, western Alboran Sea. *Journal of Geophysical Research* 104(C2):3109-3119.

Gascard, J.C. (1978). Mediterranean deep water formation baroclinic instability and oceanic eddies. *Oceanologica Acta*, 1(3): 315-330.

Gili, J.-M., Bouillon, J., Pages F., Palanques, A. and Puig, P. (1999). Submarine canyons as habitats of prolific plankton populations: three new deep-sea Hydroidomedusae in the western Mediterranean. *Zoological Journal of the Linnean Society* 125:313-329.

Gordoa, A., Illas, X., Cruzado, A., and Velásquez, Z. (2008). Spatio-temporal patterns in the north-western Mediterranean from MERIS derived chlorophyll *a* concentration. *Scientia Marina* 72: 757-767.

Hickey B.M. (1995). Coastal submarine canyons, paper presented at "Aha Huliko" A Workshop of Flow Topography Interactions, Office of Naval Research, Honolulu, 17-20 January.

Hickey, B.M. (1997). The Response of a Steep-Sided, Narrow Canyon to Time-Variable Wind Forcing. *Journal of Physical Oceanography* 27: 667-726.

Holt, J.T., Allen, J.I., Proctor, R. and Gilbert, F. (2005). Error quantification of a high-resolution coupled hydrodynamic-ecosystem coastal-ocean model: Part 1 model overview and assessment of the hydrodynamics. *Journal of Marine Systems* 57(1-2): 167 - 188. ISSN 0924-7963.

Jordi, A., Orfila, A., Basteretxea, G. and Tintoré, J. (2005). Shelf-slope exchanges by frontal variability in a steep submarine canyon. *Progress in Oceanography* 66:120-141.

Klinck, J.M., (1988). The Influence of a Narrow Transverse Canyon on Initially Geostrophic Flow. *Journal of Geophysical Research* 13(C1): 2009-515.

Klinck, J.M. (1989). Geostrophic Adjustment Over Submarine Canyons. *Journal of Geophysical Research* 94(C5): 6133-6144.

Klinck, J.M., (1996). Circulation near submarine canyons: A modeling study. *Journal of Geophysical Research* 101(C1): 1211-1223.

Kremer, J.N. and Nixon, S.W. (1978). A Coastal Marine Ecosystem: Simulation and Analysis. Ecological Studies, Vol. 24. Springer-Verlag, Heidelberg. 210 pp.

Korres, G. and Lascaratos, A. (2003). A one-way nested eddy resolving model of the Aegean and Levantine basins: implementation and climatological runs. *Annals of Geophysics* 21: 205-220.

La Violette, P. E., Tintore, J. and Font, J. (1990). The surface circulation of the Balearic Sea. *Journal of Geophysical Research* 95(C2), 1559-1568.

Lacroix, G., Ruddick, K., Park, Y., Gypens, N. and Lancelot, C. (2007). Validation of the 3D biogeochemical model MIRO&CO with eld nutrient and phytoplankton data and MERIS-derived surface chlorophyll a images. *Journal of Marine Systems* 64(1-4): 66 - 88.

Leblanc, K., Queguiner, B., Garcia, N., Rimmelin, P. and Raimbault, P. (2003). Silicon cycle in the NW Mediterranean Sea: seasonal study of a coastal oligotrophic site. *Oceanologica Acta* 26(4): 339-355. ISSN 0399-1784.

Lehmann, M.K., Fennel, K. and He, R. (2009). Statistical validation of a 3-D bio-physical model of the western North Atlantic. *Biogeosciences* 6(10): 1961-1974. ISSN 1726-4170.

López-García, M.J., Millot, C., Font, J. and García-Ladona, E. (1994). Surface circulation variability in the Balearic Basin. *Journal of Geophysical Research* 99(C2): 3285-3296.

Lotka, A. J. (1925). Elements of physical biology. Williams & Wilkins, Baltimore. [Reprinted in 1956: Elements of Mathematical Biology. Dover Publications, Inc., New York, New York].

Lucea, A., Duarte, C. M., Agustí, S. and Sondergaard, M. (2003). Nutrient (N, P and Si) and carbon partitioning in the stratified NW Mediterranean. *Journal of Sea Research* 49(3): 157 - 170. ISSN 1385-1101.

Marchesiello P., McWilliams, J. C. and Shchepetkin, A. (2001). Open boundary conditions for long-term integration of regional oceanic models. *Ocean Modelling* 3: 1-20.

Margalef, R. (1972). Interpretaciones no estrictamente estadísticas de la representación de entidades biológicas en un espacio multifactorial. *Investigación Pesquera* 36: 183-190.

Mellor, G. (2004). User's Guide for a Three-Dimensional Primitive Equation, Numerical Ocean Model. Princeton University, Princeton, N.J., 1-56

MEDOC Group (1970). Observation of Formation of Deep Water in the Mediterranean Sea, 1969. *Nature* 227:1037-1040.

Millot, C. (1990). The Gulf of Lions hydrodynamics. *Continental Shelf Research* 20: 1-9.

Millot, C. (1999). Circulation in the Western Mediterranean Sea. *Journal of Marine Systems* 20(1-4): 423 - 442. ISSN 0924-7963.

Odum, H.T. (1960). Ecological potential and analog circuits for the ecosystem. *American Scientist* 48:1-8.

Pinardi, N. and Coppini, G. (2010). Operational oceanography in the Mediterranean Sea: the second stage of development. *Ocean Science* 6: 263-267

Redfield, A. C., Ketchum, B.H., and Richards, F.A. (1963). The influence of organisms on the composition of sea water, in The Sea, edited by M. N. Hill, pp. 26– 77, Interscience, New York.

Riley, G.A., Stommel, H. M. and Bumpus, D.F. (1949). Quantitative ecology of the plankton of the western North Atlantic. *Bulletin of the Bingham Oceanographic Collection* 12(3):1–169.

Rio, M.-H., Poulain, P.-M., Pascual, A., Mauri, E., Larnicol, G. and Santoleri, R. (2007). A Mean Dynamic Topography of the Mediterranean Sea computed from altimetric data, in-situ measurements and a general circulation model. *Journal of Marine Systems* 65(1-4): 484-508. ISSN 0924-7963.

Salat, J. (1995). The interaction between the Catalan and Balearic currents in the southern Catalan Sea. *Oceanologica Acta* 18(2):227-234.

Sardà, F., Company, J. B., Bahamon, N., Rotllant, G., Flexas, M.M., Sánchez, J.D., Zúñiga, D., Coenjaerts, J., Orellana, D., Jordà, G., Puigdefábregas, J., Sánchez-Vidal, A., Calafat, A., Martín, D. and Espino, M. (2009). Relationship between environment and the occurrence of the deep-water rose shrimp *Aristeus antennatus* (Risso, 1816) in the Blanes submarine canyon (NW Mediterranean). *Progress in Oceanography* 82 (4): 227-238.

Schott, F., Visbeck, M., Send, U., Fischer, J., Stramma, L. and Desaubies, Y. (1996). Observations of Deep Convection in the Gulf of Lions, Northern Mediterranean, during the winter of 1991/92. *Journal of Physical Oceanography* 26:505-524.

Skliris, N., Goffart, A., Hecq, J.H. and Djenidei, S. (2001). Shelf-slope exchanges associated with a steep submarine canyon off Calvi (Corsica, NW Mediterranean Sea): A modeling approach. *Journal of Geophysical Research* 106(C9):19,883-19,901.

Steele, J.H. (1970). Marine food chains (Ed). University of California Press, Berkeley, 552 pp.

Sorgente, R., Drago, A.F. and Ribotti, A. (2003). Seasonal variability in the Central Mediterranean Sea circulation. *Annals of Geophysics* 21: 299-322.

Thingstad, T.F., Zweifel, U.L. and Rassoulzadegan, F. (1998). P limitation of heterotrophic bacteria and phytoplankton in the northwest Mediterranean. *Limnology and Oceanography* 43: 88–94.

Tonani, M., Pinardi, N., Dobricic, S., Pujol, I. and Fratianni, C. (2008). A high-resolution free-surface model of the Mediterranean Sea. *Ocean Science* 4, 1-14

Tonani, M., Pinardi, N., Fratianni, C., Pistoia, J., Dobricic, S. Pensieri, S., de Alfonso, M. and Nittis, K. (2009). Mediterranean Forecasting System: forecast and analysis assessment through skill scores. *Ocean Science* 5, 649-660.

Varela, R.A., Cruzado, A., Tintoré, J. and García-Ladona, E. (1992), Modelling the deep-chlorophyll maximum: A coupled physical-biological approach. *Journal of Marine Research* 50:441-463

Varela, R.A., Cruzado, A., Tintoré, J. (1994). A simulation analysis of various biological and physical factors influencing the deep chlorophyll maximum structures in oligotrophic areas. *Journal of Marine Systems* 5: 143-157.

Varela, R.A., Cruzado, A., Gabaldon, J.E. (1995). Modelling primary production in the North Sea using the European Regional Seas Ecosystem Model. *Netherlands Journal of Sea Research* 33(3): 337-361.

Vargas-Yáñez, M., Zunino, P., Benali, A., Delpy, M., Pastre, F., Moya, F., García-Martínez, M.C. and Tel, E. (2010). How much is the western Mediterranean really warming and salting*? Journal of Geophysical Research* 115: doi:10.1029/2009JC005816.

Velasquez, Z.R. (1997). Phytoplankton in the NW Mediterranean. *Ph.D. Thesis*, UPC, Barcelona, pp. 272.

Vetter E.W., Smith, C.R. and De Leo, F.C. (2010). Hawaiian hotspots: enhanced megafaunal abundance and diversity in submarine canyons on the oceanic islands of Hawaii. *Marine Ecology* 31: 183-199. ISSN 0173-9565.

Vichi, M. (2000). The influence of high-frequency surface forcing on productivity in the euphotic layer. Biological Observations in Operational Oceanography. EuroGOOS Publication Nº 15. EuroGOOS Office, Southampton.

Volpe, G., Nardelli, B.B., Cipollini, P., Santoeri, R., and Robinson, I.S. (2011). Seasonal to interannual phytoplankton response to physical processes in the Mediterranean Sea from satellite observations. *Remote Sensing of Environment*, doi:10.1016/j.rse.2011.09.020.

Volterra, V. (1926). Variazioni e fluttuazioni del numero d'individui in specie animali conviventi. Mem. R. Accad. Naz. Dei lincei. Ser. VI (2). [Translated into English by M. E. Wells 1928, *Journal du Conseil International pour l'Exploration de la Mer* 3: 1–51.]

Wroblewski, J.S., Sarmiento, J.L., Flierl, G.R. (1988). An ocean basin scale model of plankton in the North Atlantic. Solutions for the climatological oceanographic conditions in May. *Global Biogeochemical* Cycles 2: 199-218.

Wroblewski, J.S. (1989). A model of the spring bloom in the North Atlantic and its impact on ocean optics. *Limnology and Oceanography* 34: 1565-1573.

Zavatarelli, M. and Pinardi, N. (2003). The Adriatic Sea modelling system: a nested approach. *Annals of Geophysics* 21: 345-364.